PCCP

Accepted Manuscript

ROYAL SOCIETY OF CHEMISTRY

www.rsc.org/pccp

Pinacyanol Chloride Forms Mesoscopic H- and J-Aggregates in Aqueous Solution – A Spectroscopic and Cryo-Transmission Electron Microscopy Study

Hans v. Berlepsch,* Kai Ludwig and Christoph Böttcher

Forschungszentrum für Elektronenmikroskopie, Institut für Chemie und Biochemie, Freie Universität Berlin, Fabeckstraße 36a, D-14195 Berlin, Germany

Abstract

The aggregation behaviour of the cationic pinacyanol chloride in aqueous solution is investigated by absorption and linear dichroism spectroscopies, optical microscopy and cryogenic transmission electron microscopy (cryo-TEM). The investigations are focused on solutions in a concentration range from 50 μM up to 1 mM. At a concentration of 0.7 mM H-aggregates are detected that are characterized by a broad absorption band centred at ~ 511 nm. The aggregates possess a tubular architecture with a single-layer wall thickness of ~ 2.5 nm and an outer diameter of ~ 6.5 nm. Linear dichroism spectroscopy indicates that the molecules are packed with their long axis parallel to the tube axis. These H-aggregates are not stable, but transform into J-aggregates on the time scale of weeks. The kinetics of J-aggregation depends on the dye concentration and the route of sample preparation, but can also be enhanced by shear stress. J-aggregates possess a split absorption spectrum composed of two longitudinally polarized J-bands and one H-band that is polarized perpendicular to the aggregate axis. The J-aggregates are ~ 9 nm wide and several micrometer long fibrils consisting of stacked pairs of ribbons with dumbbell-shaped density cross-section. Upon aging these ribbons unilaterally stack face-to-face to form tape-like aggregates.

1. Introduction

Self-aggregation in polar environment is a common phenomenon of dye molecules possessing extended planar π-electron systems. Directly related to such aggregation process is a dramatic change of the optical properties due to dipole-dipole coupling between the transition dipole moments of neighbouring molecules. The interactions lead to new electronic excitations, Frenkel excitons, that are delocalized over a range of molecules rather than localized on an individual molecule.[1] In dependence on the spatial orientation of dipoles relative to the aggregate axis, two types of absorption spectra are commonly observed, namely such, where the aggregate absorption band is red-shifted with respect to the monomer absorption band and such exhibiting a shift to the blue side (hypsochromic shift) of the monomer spectrum.[2-4] The assemblies of the first kind have been named Jelly (J-) or Scheibe aggregates in honour of their discoverers,[5,6] the second kind were denoted H-aggregates, because of the characteristic hypsochromic band shift. Due to their peculiar spectroscopic properties dye aggregates have become commercially important as spectral sensitisers in imaging technology[7] and they have large potential for applications in the fields of opto-electronics, non-linear optics,[8] or bioanalytics.[9,10]

The prototypical and to this day most widely studied cyanine dye forming molecular aggregates by self-assembly in aqueous solution is pseudoisocyanine chloride (1,1'-diethyl-

2,2'-cyanine chloride, PIC-Cl). Pinacyanol chloride (1,1'-diethyl-2,2'-carbocyanine chloride, PCYN-Cl, Chart 1) is a homologue to PIC and differs from that only in the length of the alkene bridge between the two quinoline moieties, which is longer by two methine units for PCYN. PCYN has been used as a redox indicator to monitor peroxide activation,[11] a saturable absorber, mode-locker, sensitiser in imaging technology,[12,13] a diagnostic tool for the study of polysaccharides,[14-16] to determine physicochemical properties of micelles[17,18] and vesicles,[19] as well as to probe fibrillization of β-amyloid peptide.[20]

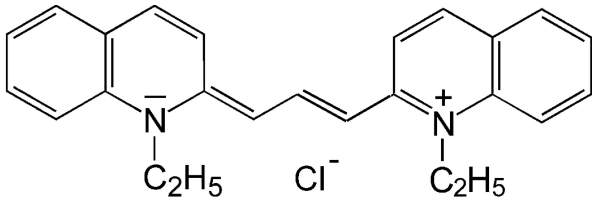

Chart 1 Molecular Structure of Pinacyanol Chloride

Most of the applications of PCYN utilize the strong binding of the cationic dye to anionic colloids, which promotes aggregation.[21,22] Aggregation causes a blue-shift of the absorption band due to the formation of dimers[23] and higher H-type aggregates.[22] In contrast to PIC-Cl, which shows very strong J-aggregation, the evolution of J-aggregates for PCYN was in fact supposed in a few studies,[18,22,24] but until now not conclusively demonstrated.

The self-aggregation behaviour of PCYN-Cl in ethanol-water solutions was recently investigated in detail by Khouri *et al*.[25] Monomers, different species of dimers, higher aggregates, as well as several vibronic bands were identified by linear absorption spectroscopy. The Kauffmann group studied the monomer-dimer equilibrium by two-dimensional electronic spectroscopy,[26] as well as the high frequency vibrational modulations in the two-dimensional electronic spectra of monomers.[27] In all the mentioned investigations the chosen dye concentration was fairly low.

Despite broad exploitation of the aggregates' photophysical properties the physical structure of dye aggregates is often insufficiently characterized. This is in particular valid for the aggregates of PCYN and in part related to the suspected smallness of aggregates. An increase of the dye concentration should stimulate the growth of aggregates and could thus help promoting structure characterization. Following this concept we surveyed the PCYN literature and found only one study of Tiddy's group,[28] dealing with higher concentrated dispersions. The study was focused on the usability of prospective chromonic liquid

crystalline phases of PCYN-Cl as template for the preparation of mesoporous solids. The experiments were unsuccessful, however, because the dye chloride appeared not sufficiently soluble, but precipitated instead of forming liquid crystals. To improve the water-solubility these researchers exchanged the chloride by acetate anions and, indeed, observed the formation of nematic and hexagonal liquid crystals from ~ 18 mM solutions. SAXS measurements revealed that the aggregates forming the mesophases are single-walled nanotubes with an outer tube diameter of 4.6 nm. Due to the blue-shifted absorption maximum[28] the aggregates can be classified as H-aggregates.

In this context we wondered what type and supramolecular structure of aggregates the PCYN chloride salt would form at high concentration. Prior to a structural characterization the solutions were thoroughly characterized by absorption spectroscopy to correlate the optical properties with the particular preparation conditions and to evaluate the optimal experimental conditions under which the dye forms stable aggregates suitable for a morphological characterization. For that we used cryogenic transmission electron microscopy (cryo-TEM), a technique that provides highly resolved direct images of colloidal aggregates in their native environment[29] and has routinely been used in recent years for the characterization of the microstructure of several types of cyanine dye aggregates on the nanometre-to-micrometer scale.[30]

2. Experimental

PCYN-Cl was supplied by Sigma-Aldrich and was used as received. The molar extinction coefficient in ethanol was found to be $\varepsilon = 1.75 \times 10^5$ dm^3 mol^{-1} cm^{-1}. In standard conditions the required amount of dye was directly dissolved by stirring in Milli-Q water (conductivity < 1 μS cm^{-1}) for one day at room temperature. Heating was not necessary because of the high water solubility of the dye for concentrations up to at least 10 mM. In addition to this direct route of preparation also samples were prepared by diluting a 10 mM stock solution with Milli-Q water (dilution route).

Isotropic absorption spectra were measured with a Cary 50 spectrophotometer (Varian). Linear dichroism (LD) spectra were measured with a J-810 spectropolarimeter (Jasco Corp.) by using a Dioptica microvolume Couette flow LD cell (Dioptica Scientific Limited, Rugby, Warwickshire, UK) with 0.5 mm optical path length.[31] In order to acquire a complete LD spectrum shear was applied for 1.5 min. The LD measurements were carried out at 25 °C, all other spectroscopic measurements at room temperature (21 ± 1 °C).

The optical microscope images were obtained by using a colour video camera (Model TK-1070E, JVC) set on an optical microscope (Model BH-2, Olympus) equipped with Phase Contrast Attachment (Model BH2-PC). The samples were prepared by placing a droplet of the solution on a microscope slide and protected against drying by a cover glass.

The samples for cryo-TEM were prepared at room temperature by placing a droplet (5 μL) of the solution on a hydrophilized (60 s Plasma treatment at 8 W using a BALTEC MED 020 device) perforated carbon filmed Quantifoil (Jena, Germany) grid. The excess fluid was blotted off to create an ultrathin layer (typical thickness of 100 nm) of the solution spanning the holes of the carbon film. The grids were immediately vitrified in liquid ethane at its freezing point (–184 °C) using a standard plunging device. Ultrafast cooling is necessary for an artefact-free thermal fixation (vitrification) of the aqueous solution avoiding crystallization of the solvent or rearrangement of the assemblies. The vitrified samples were transferred under liquid nitrogen into a Philips CM12 transmission electron microscope using the Gatan cryo-holder and -stage (Model 626). Microscopy was carried out at –173 °C sample temperature using the microscopes low dose protocol at a primary magnification of 58300 ×. Under standard conditions the defocus was chosen to be 1.3 μm, which corresponds to a first zero of the phase contrast transfer function (CTF) at 2.2 nm. Some micrographs were taken at a reduced defocus of 0.6 μm with a respective first zero of the CTF at 1.7 nm.

3. Results and Discussion

3.1. Spectroscopic Characterization

The dashed line in Fig. 1 represents the normalized absorption spectrum of a 1.0×10^{-5} M PCYN-Cl solution in water, which is basically identical with the dye monomer spectrum in ethanol (see ESI† S1) where dye aggregation can be excluded. The main absorption band centred at 600 nm corresponds to the $0 \rightarrow 0$ transition, whereas the second maximum at 555 nm and the shoulder at ~ 515 nm can be assigned to vibrational sub-bands. This behaviour is typical for many different cyanine dyes.[32] A set of normalized absorption spectra is added to Figure 1, which was measured after progressive dilution of a fresh 1.0 mM PCYN-Cl solution with water. The 1.0 mM starting solution prepared by the direct route (see Experimental) shows bands at around 600 nm, 544 nm, and 511 nm, whereat the longest wavelength band can be assigned to residual monomers and the both others to different sorts of aggregates, respectively. With decreasing dye concentration the shortest wavelength band decreases in intensity and shifts to the red, whereas the shoulder at around 544 nm becomes a clearly resolved peak. In addition, the monomer band at 600 nm grows.

The detected changes of absorbance as a function of concentration are widely in accordance with the findings of Khouri and Buss,[25] who have investigated the spectral behaviour of aqueous PCYN-Cl solutions containing 7.5 % (v/v) ethanol in more detail. Using derivative spectroscopy these authors resolved different H-bands and assigned them to various dimer species coexisting in equilibrium. One particular band centred at 507 nm turned out to represent an exceptional case. It increased linearly with the concentration, *i.e.* it did not show any levelling off, which would be expected if there were a significant dissociation of aggregates and rearrangement into larger aggregates. This peak has been assigned to trimers or higher aggregates. The pronounced H-band that we detected in pure water at 511 nm obviously corresponds to this 507 nm band in the water-ethanol mixture. The adsorption of PCYN on negatively charged colloids results in similar H-type aggregation. These aggregates do not exhibit any noticeable fluorescence under visible light excitation,[12] which is another typical feature of H-aggregates besides the blue-shift of the absorption band.[2] Photophysical properties of these species were also measured and support the assignment.[12]

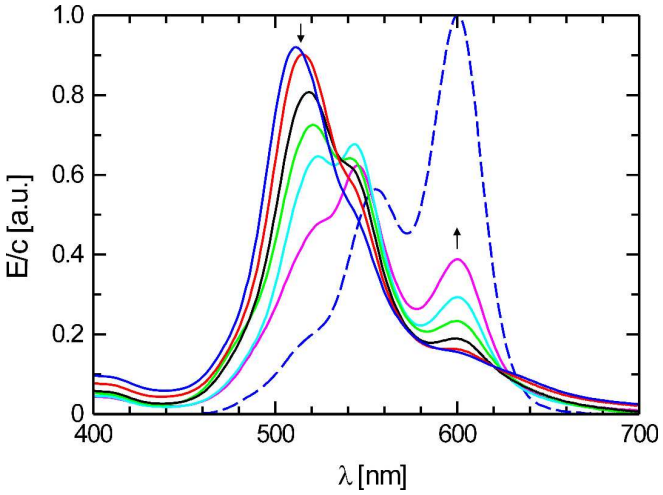

Fig. 1 Concentration dependent absorption spectra of aqueous PCYN-Cl solutions. The curves were measured after progressive diluting (indicated by arrows) with water. The extinction, E, is normalized by the respective dye concentration, c. c (in mM) = 1.0, 0.7, 0.35, 0.21, 0.10, 0.05. The dashed line represents the normalized monomer absorption spectrum obtained for a 1.0×10^{-5} M solution in water.

For many applications it is sufficient that a dye solution is stable over only a few days. Because in the self-assembly of molecular systems (including dyes) a multitude of molecular interactions often compete for an equilibrium structure, long-time kinetics is normally observed.[33] For amphiphilic dyes, in particular,[34] it can arise from structural transformations between different types of aggregates or morphologies. Looking for similar structural changes we followed the absorbance of PCYN-Cl solutions during their storage at room temperature in

the dark over a period of months. Within the first few days after preparation solutions of 1 mM did not show marked changes in absorbance. Over the following weeks the absorbance, however, changed, as depicted for a representative example in Fig. 2. On the first sight the long-time storage seemingly marked a bleaching of the solution only. Scaling up the long wavelength tail, however, revealed distinguishable absorption bands evolving at wavelengths around 600 and 650 nm, though the effect appears to be rather small. Similarly weak bands emerged upon the interaction of PCYN with polymers,[15,22] β-amyloid fibrils[20] or micelles of the cationic surfactant sodium bis (2-ethylhexyl) sulfosuccinate (Aerosol-OT) in aqueous solutions.[18] Also aqueous PCYN iodide solutions containing 200 mM NaCl showed similar bands.[24] Due to their general appearance on the long-wavelength side of the monomer spectrum they were ascribed to J-aggregates.[22]

In a second experiment the absorbance of a 1.0 mM solution prepared by the dilution route (from a 10 mM stock solution) was followed over several months. Surprisingly, much stronger spectral changes became visible here as depicted in Fig. 3. The 511 nm band weakened again, while the absorbance in the long-wavelength region markedly increased. In particular, the weak shoulders at 600 nm and 650 nm became clearly resolved maxima. The

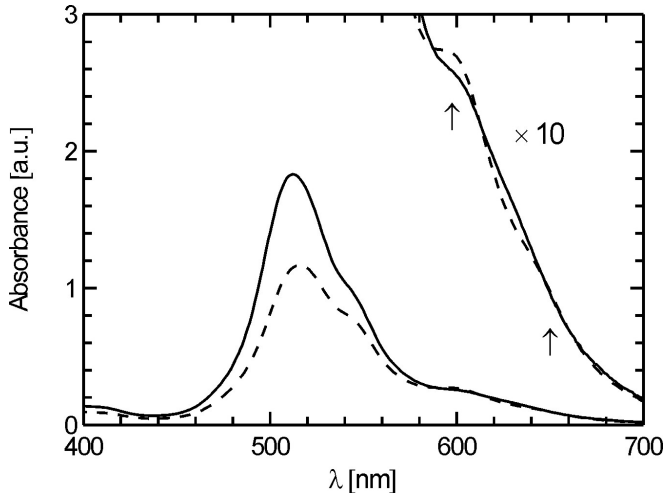

Fig. 2 Changes of absorbance of a sample prepared by the direct route during long-time storage. Absorbance of a 1.0 mM PCYN-Cl solution after one day (solid) and after 6 weeks of storage in the dark (dash). The enlarged long-wavelength part of the spectrum reveals slightly increasing absorbance at around 600 and 650 nm (indicated by arrows).

absorbance at around 550 nm remains largely the same but an additional hump evolved at around 480 nm. The spectral changes are qualitatively consistent with those discussed in the context of Fig. 2, but are strongly enhanced here. The enhancement of the 600 nm band cannot be attributed to an increase in the concentration of monomers, because de-aggregation

during storage under unchanged solvent conditions seems rather unlikely. Instead, the changes suggest the formation of a novel type of aggregate. The absorption spectrum of these aggregates can be estimated by subtraction of the spectrum recorded of a freshly prepared solution from that recorded after seven months. The result is plotted as dotted line in Fig. 3. A remarkable outcome is the appearance of an additional H-band at ~ 490 nm. Due to its splitting into one H-band (490 nm) and two J-bands (600 and 650 nm), as well as the enormous spread completely covering the spectrum of monomers, the spectrum points to a J-aggregate of complex molecular structure. One should note, however, that based on these kinetic data alone it cannot be excluded that the resolved sub-bands belong to different species of aggregates coexisting in the solution.

It is interesting to compare the present findings with those of Min *et al*.[24] who investigated aqueous PCYN-I solutions. In the presence of 200 mM NaCl they found a similar new type of aggregate. Using a comparable deconvolution procedure they estimated an absorption spectrum composed of a J-band at 640 nm and an H-Band at 471 nm. Fluorescence could be detected neither at 640 nm nor at 471 nm excitation. The authors suggest that the new type of aggregate is formed by the aggregation of dimers adopting an intermediate geometry between parallel and head-to-tail orientations.

To explain the quantitative differences of absorption spectra displayed in Figs. 2 and 3 the sample history is important. Thus, it must be taken into account, that although the concentrations of both samples were identical (1 mM), the samples were prepared by different routes. The present investigations suggest that the aggregates formed upon increasing the dye concentration do not completely dissolve if the solution is again diluted to the start concentration, *i.e*. the dissociation of the aggregates seems kinetically inhibited. The aggregates surviving the dilution step within the time scale of experiment can act as nuclei, seeding the formation of new aggregates. Because we didn't include an additional heating step after dilution favouring de-aggregation of remaining aggregates, it seems rather likely that such mechanism became operative for the dilution preparation route. At the present stage of knowledge a more quantitative discussion, however, is not possible. Nevertheless, a porphyrin-based dye system where the H-aggregation is initiated upon the addition of aggregate seeds has recently been analysed through a biomimetic approach.[35] The aggregation process is quantitatively described as an "artificial infection" process in which the dye monomers assemble into nanoparticles, and are then converted into fibres in the presence of an aliquot of the nanofibre, which acts as a "pathogen". The authors suggested that their

system is not a special case, but that similar systems can be established in other metastable supramolecular assemblies exhibiting autocatalytic processes.

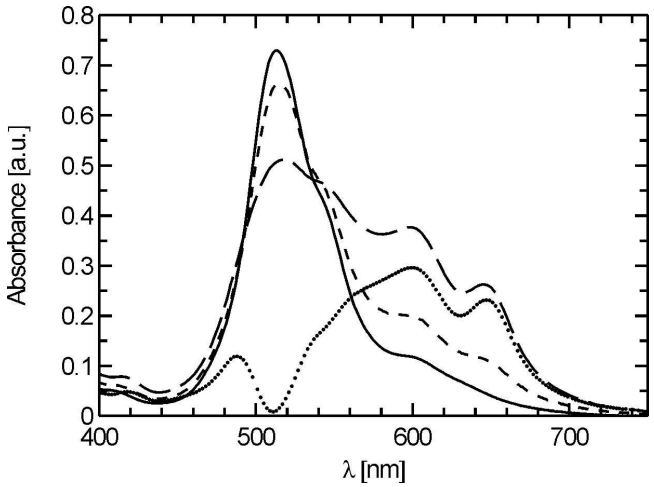

Fig. 3 Aging behaviour of a 1.0 mM PCYN-Cl solution prepared by the dilution route (starting at 10 mM stock solution). Displayed are the absorption spectra measured within 1 day (solid), 1 month (short dash), and 7 months (long dash) after dilution. The dotted curve was obtained by subtraction of the spectrum measured after 1 day (and normalized to the same peak value at 511 nm) from that measured after 7 months of storage.

Polarized absorption spectroscopy is a highly sensitive method that can give valuable information about the packing orientation of monomers within molecular aggregates and the pathway of aggregation.[36] According to the morphological investigations (discussed below) the present J-aggregates are linear objects characterized by a large aspect ratio. Thus, a preferential alignment of the aggregates by the streaming field in a Couette flow cell parallel to the flow direction could be expected. Fig. 4a presents a set of absorption spectra (monitored by the HT-channel of the spectropolarimeter), taken under shear flow at different rotation speeds for a 6-weeks-old 1.0 mM PCYN-Cl sample. Figure 4b shows the corresponding LD spectra. The absorption spectra remain nearly unchanged under different shear rates and show the typical spectral features of a 1.0 mM dye solution measured at rest state (solid line in Fig. 3), *i.e.* showing a strong H-band centred at 511 nm and weak shoulders at around 544 and 600 nm, respectively. As expected, the LD signal is nearly zero at rest. Drastic changes, however, appeared for the linear dichroism as a function of rotation speed. Up to 2000 rpm (shear forces of ~ 1200 s^{-1}) the LD spectra appeared very similar to the typical absorption spectrum. The positive sign of the LD-band centred at ~ 500 nm indicates that it is polarized parallel to the long axis of aggregates, *i.e.* the constituent molecules can be considered to be oriented with their long axis mainly parallel to this direction. Upon further increase of rotation speed

two new LD bands evolved at ~ 600 nm and 640 nm, the band at 500 nm became weaker, and a kink appeared at ~ 480 nm. These detected changes in the LD spectra again point to the formation of a novel type of aggregate, here obviously induced by application of shear stress.

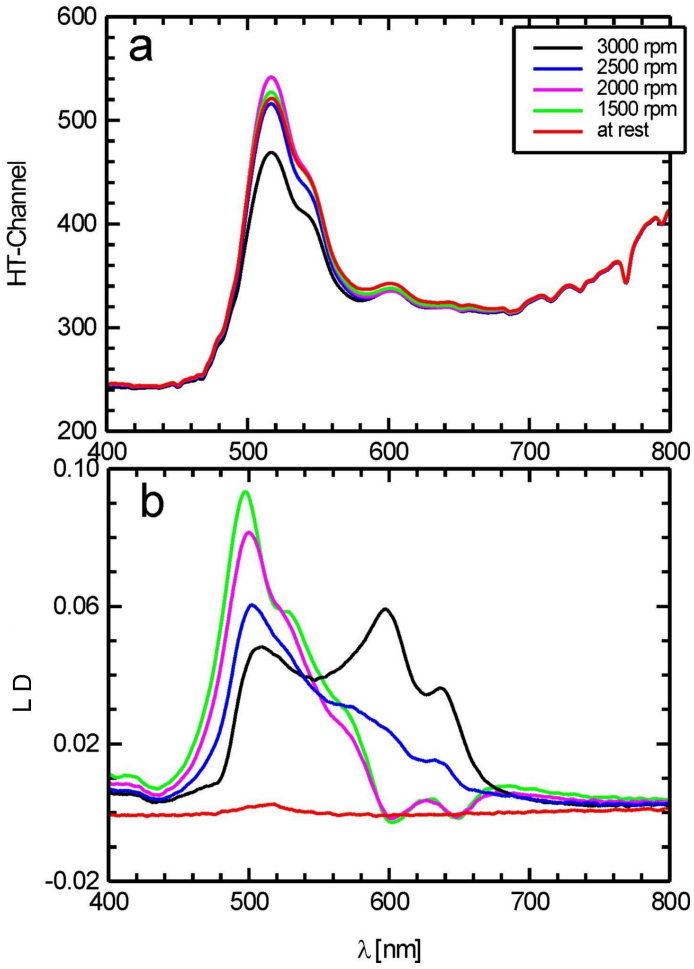

Fig. 4 Structure transformation of a 6-weeks-old 1.0 mM PCYN-Cl solution induced by shearing in a Couette flow cell. (a) The HT-channel of the spectropolarimeter monitors the absorbance of the sample as function of rotation speed. (b) Collected LD spectra as function of rotation speed. Up to 2000 rpm a broad positive band extending from 460 to 600 nm dominates LD. Upon the further increase of rotation speed the band becomes weaker and new ones appear at 600 nm and 640 nm. In addition, a kink evolves at around ~ 485 nm.

The structural investigations on sheared solutions support the observations (for a TEM micrograph see ESI† S2). After the measurement the sample showed some precipitated material. Mechanical flocculation induced solely by interfibre friction in flowing fibre suspensions is a well-known phenomenon.[37] Such mechanism could have mediated the transformation of one type of aggregate into another one and is presumably also responsible for precipitation of part of the dye material. Shear stress can also induce phase transitions in

complex fluids by lowering the energy barrier for nucleation and by accelerating the growth of a stable phase from a metastable one.[38]

To learn more about the flow instability of aggregated dye solutions we repeated the shear experiment with a 1-day-old 0.7 mM solution, i.e. at slightly lower dye concentration. Note that 0.7 mM solutions did not show any indication for a structural transformation, even after several months of storage. A summary of the spectroscopic results is depicted in Fig. 5, whereas the complete set of spectra can be found in the supporting information (see ESI† S3). Absorption spectra (left ordinate) measured at rest before applying shear (solid line) and after shearing (long dashes) are displayed in Fig. 5. Added is the difference spectrum (short dashes) calculated after normalizing both curves to the same amplitude at 514 nm. The latter spectrum

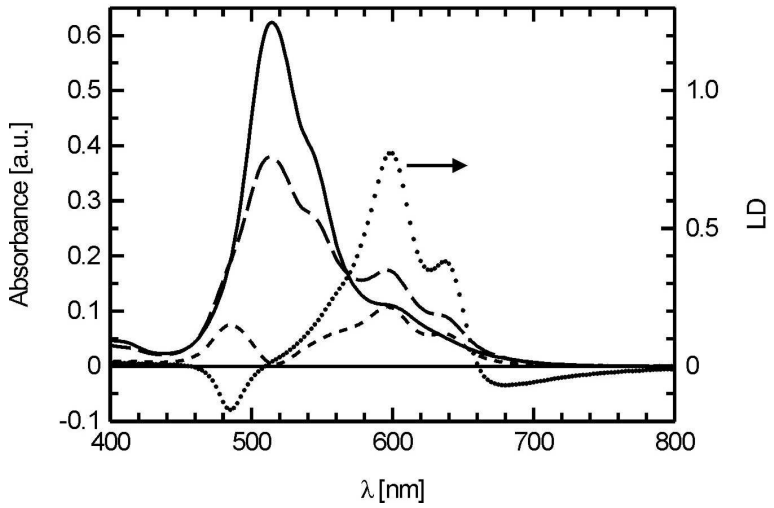

Fig. 5 Absorption spectra (left ordinate) of a 0.7 mM PCYN-Cl solution measured at rest after one day of preparation before shearing (solid) and after shear was applied for 1.5 minutes in a Couette flow cell at 2000 rpm (long dash). The difference spectrum (short dash) calculated after normalization to the same amplitude at 514 nm reveals new absorption bands at 485, 597, and 639 nm. The dotted line (right ordinate) represents the LD spectrum obtained at a rotation speed of 2000 rpm.

reveals new absorption bands with peaks at 485, 597, and 639 nm and agrees almost perfectly with that displayed in Fig. 3 (dotted line), which was derived by a similar deconvolution procedure from the aging experiment. The intensity of the detected LD signal increased with the rotation speed before at 3000 rpm saturation was reached. Thereby the shape of spectra remained almost unchanged (see ESI† S3). The dotted line in Fig. 5 represents the LD spectrum for a rotation speed of 2000 rpm. The well resolved LD bands, i.e. a negative one centred at ~ 485 nm and two positive ones centred at 597 nm and 639 nm, match exactly those of absorbance. The signs of LD bands indicate that the 485 nm band is polarized perpendicular to the aggregate axis, while the others are polarized parallel to the aggregate axis. A

similar polarization behaviour is known for other dye aggregates with Davydov split transitions as well,[39] but the issue seems more complex here, because two parallely polarized bands exist. Nevertheless, the fact that aging and shearing experiments give similar spectra clearly speaks for the formation of a single type of new aggregate, rather than for the formation of several coexisting species. Further support comes from the structural investigations. Finally, it is worth mentioning that is not fully clear, why the fresh 0.7 mM sample (ESI† S3), possesses a markedly reduced stability against shearing compared to the matured 1.0 mM sample (Fig. 4a), but in any case this finding underlines once again the sensitivity of spectroscopic behaviour to the sample history.

3.2. Morphology of Aggregates

Cryo-TEM can provide structure information of dye aggregates on the nanometre scale in the native aqueous environment. We started our investigations with a 0.35 mM sample showing absorption bands in the short-wavelength region at 518 nm and 544 nm (see Fig. 1). For this sample we did not find assembly structures. Expected oligomers were obviously too small to be identified via cryo-TEM supporting earlier investigations.[30] At a concentration of 0.7 mM with the H-band shifted to 511 nm, however, linear aggregates became clearly visible. A representative micrograph shown in Fig. 6a reveals individual aggregates of 100 to 200 nm length and a horizontally striped background pattern. The appearance of a pair of parallel dark lines is characteristic for the individual aggregates and points to a tubular morphology. The wall thickness is about 2.5 nm and the outer tube diameter amounts to about 6.5 nm. Fig. 6b shows overlaid line scans across 12 individual aggregates. The derived profile is typical for a hollow cylindrical structure and proves that the aggregates are indeed nanotubes.

The analysis of many cryo-TEM micrographs reveals that the stripes forming the background pattern are uniformly oriented in single domains, which extend over few hundreds of nanometres. Neighboured domains in general possess different orientations. The Fourier transform of cryo-TEM images (see ESI† S4) yields a repetition period of stripes of about 6.5 nm. This value suggests that the stripes are views of large ensembles of tightly packed individual tubes forming well-ordered domains. Fig. 7a shows a small section from a large domain at high magnification. The derived density profile across the pattern depicted in Fig. 7c yields for the width of stripes and their repetition period values of ~ 5 nm and ~ 6.5 nm, respectively. These data are consistent with a model of tightly packed individual tubes sketched in Fig. 7b. Note that the width of an individual stripe amounts to approximately twice the thickness of the tube wall (2.5 nm). Moreover, a small density dip is often seen in

the centre of the stripes (Fig. 7c), where two neighboured tubes are in contact. The shearing of the samples associated to its blotting during specimen preparation[40] is most likely the reason for the alignment of tubes. Tiddy *et al*.[28] observed for the PCYN acetate with increasing concentration first a nematic (N phase) and thereafter a hexagonal liquid crystalline phase (M phase). From SAXS measurements it was inferred that the elongated aggregates forming the mesophases are tubes with a diameter of 4.6 nm. Thus, we obtain a quite similar result for the present chloride PCYN salt.

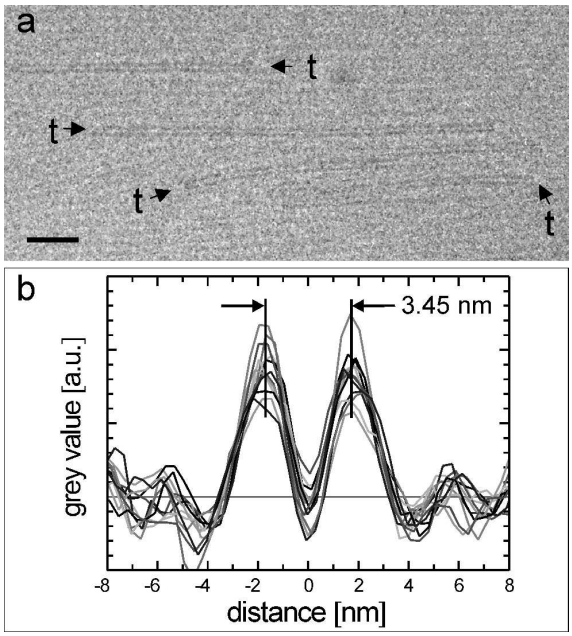

Fig. 6 Cryo-TEM micrograph of a 0.7 mM PCYN-Cl sample two days after preparation. Panel (a) shows several isolated tubules (t) and a horizontally oriented striped background. Bar = 30 nm. Panel (b) shows line scans across 12 individual tubular aggregates. The external diameter of tubules is ~ 6.5 nm, their wall thickness ~ 2.5 nm.

The wall thickness determined from the density profiles is ~ 2.5 nm and points to a monolayer arrangement of dye molecules.[30] Due to experimental difficulties (possible interference effects; the averaging was done over a highly curved layer) the true wall thickness can be somewhat smaller, but a bilayer arrangement can surely be excluded. To explain the blue-shift of the absorption band (centred at 511 nm) adjacent molecules should be placed on top of each other, or with only a small relative shift (*i.e.*, side-by-side orientation typical for H-aggregates). The parallel polarization of the absorption band indicates that the molecules are preferentially oriented with their long axis parallel to the tube axis. This packing structure would differ from the hollow brickwork chimney model proposed by Tiddy *et al*.,[28,41] where the molecules are assumed to be perpendicularly oriented.

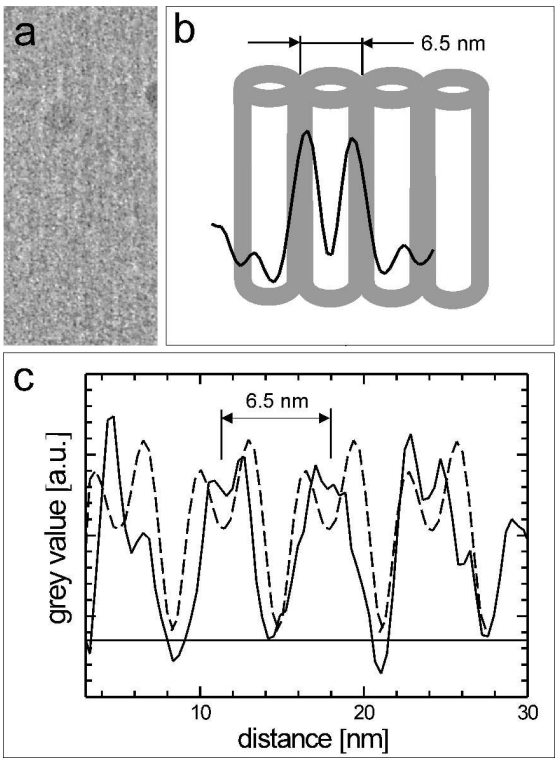

Fig. 7 The close parallel packing of individual tubes into ordered domains can explain the striped background pattern. (a) Cryo-TEM micrograph showing the background pattern at high magnification. Bar: 20 nm. (b) Packing motif of four individual tubes together with the averaged density profile of a single tube as black line. (c) Experimental density profile (solid line) derived from the cryo-TEM image in panel (a) and simulation by superimposing individual tube profiles taken from (b) (dashed line).

Complementary to electron microscopy we studied the solutions by optical microscopy. In fresh preparations of 1 mM PCYN-Cl solutions with a typical H-band at 511 nm no structures could be detected. We surmise that tubular H-aggregates cannot be resolved by optical microscopy. After about one week of storage thread-like fibres, however, became visible. After some weeks the absorbance (see Fig. 2) indicated the formation of J-aggregates and the number of assemblies strongly increased. The number of fibres was markedly higher for solutions prepared by the dilution route (Fig. 8) if compared with a directly prepared 1 mM sample. This observation supports our earlier conclusions of the sample history-dependence (Figs. 2 and 3). Also samples at 0.7 mM concentration showed fibres, but significantly smaller in number and not before several month of storage. All these fibres were thread-like, flexible, and many tens of micrometers long. Needle-like crystals[42] were not observed. The morphological characteristics and the distinct kinetic effects suggest that these fibres represent the evolving species of J-aggregates. Due to the limited resolution of light

microscopy structural details could not be obtained. High resolution TEM data are presented in the following section.

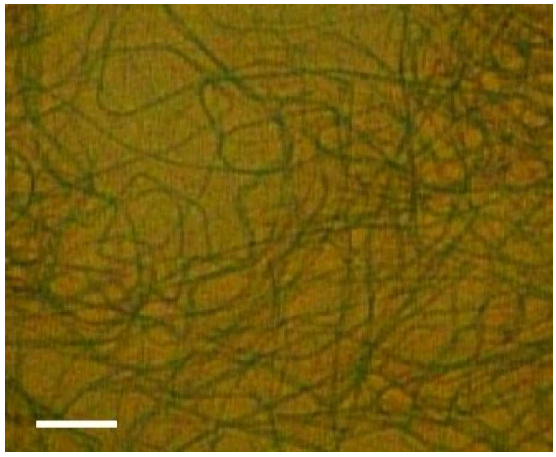

Fig. 8 Fibrous J-aggregates visualized by optical microscopy (transmission mode) of a 1.0 mM PCYN-Cl solution. The image was taken three weeks after dilution from a 10 mM sample. Bar: 10 µm.

A representative cryo-TEM image of a 1.0 mM PCYN-Cl solution revealing slightly bent fibrillar aggregates is shown in Fig. 9. The fibres possess a non-circular cross-section as is evident from the changing width if one follows an individual fibre along its axis. The assembly of such individual fibrils into larger assemblies occurs upon long-time storage of samples and is described below in more detail.

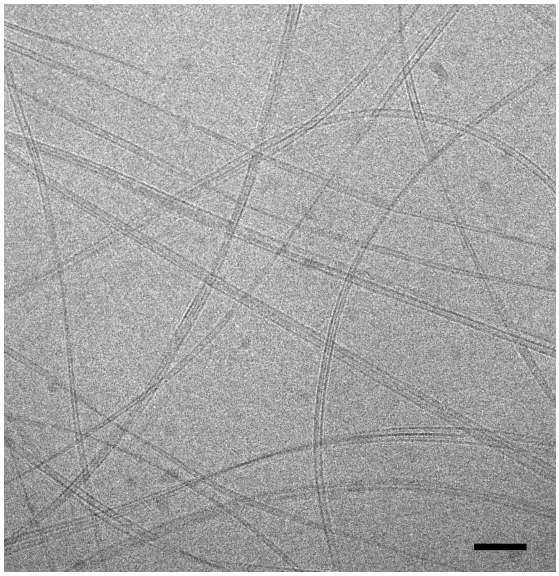

Fig. 9 Cryo-TEM micrograph of a 1.0 mM PCYN-Cl solution taken 4 days after dilution from a 10 mM sample. Bar: 50 nm.

In Fig. 10a a cryo-TEM image of a typical unbent fibril is shown. The width and the structural pattern change periodically along the fibril axis, which is a typical phenomenon observed with twisted layered ribbon structures. One repetition period of the fibril corresponding to a 180° rotation is presented in the image. Line scans taken perpendicular to the fibrils' long axis in the crossover position (0°) and halfway between two adjacent crossover points, *i.e.* at 90°, are presented in Figs. 10b and 10c, respectively. Based on these observed profiles we propose the structure model displayed in Fig. 10d. The model suggests the fibril to consist of a pair of ribbons with dumbbell-shaped density cross-sections, a two-fold rotational symmetry and a regular twist around the fibril long axis. To check the proposed model we compared the image data with the corresponding simulated projection image of the model (Fig. 11). As a matter of fact the complex angle-dependent pattern is well reproduced by the simulation.

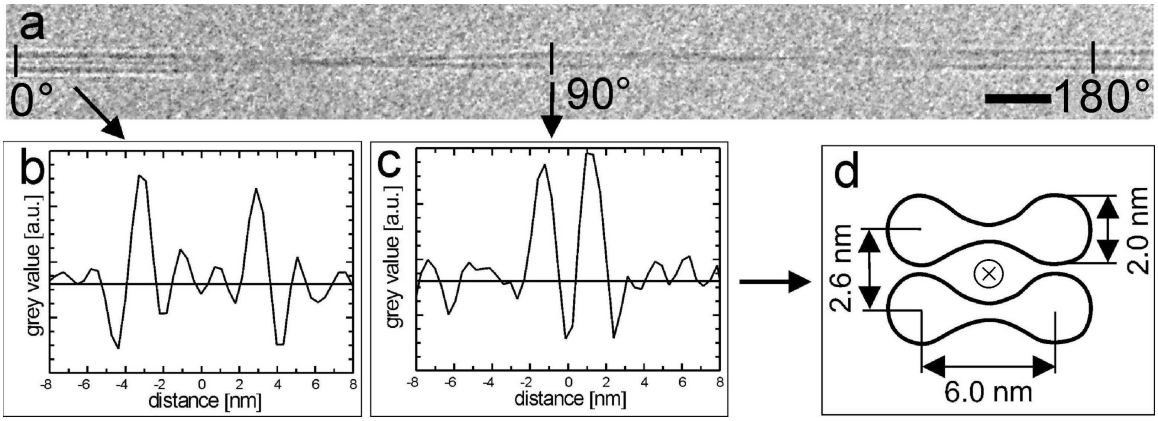

Fig. 10 (a) Representative cryo-TEM micrograph of an unbent single J-aggregate revealing a twisted ribbon morphology. The distance between two adjacent crossovers equals half the pitch of the fibril and corresponds to a rotation of 180°. The pitch is about 1 μm but its value can vary between individual fibrils. The striped background pattern can be assigned to coexisting tubular H-aggregates. Sample: 1.0 mM PCYN-Cl solution vitrificated two weeks after dilution from a concentrated (10 mM) sample. Bar: 25 nm. Panels (b) and (c) show line scans taken across the fibrils' long axis in the crossover position (0° orientation) and in the centre between two adjacent crossover points (90° rotation). The estimated grey value profile along the fibril suggests a structure (panel d) consisting of a pair of ribbons with dumbbell-shaped density cross-sections that are stacked face-to-face and twisted around the fibril axis (marked by ⊗).

Dye aggregates consisting of ribbons with homogeneous thickness have frequently been observed. Often their width increases by aging. Also the stacking of single ribbons into double- and multilayered structures is well known.[30] However, in the case at hand a different architecture is adopted. The ribbon appears to consist of two ~ 2 nm thick strands that are kept

at a distance of ~ 6 nm by a thinner bridge, which generates a dumbbell-shaped cross-section in the images. The interlayer spacing is about 2.6 nm. The stacking of ribbons is indicative of strong attractive intermolecular forces. The analysis of many individual fibrils shows that the constituent ribbons have throughout identical width. Individual ribbons were never observed. By analysing several tens of cryo-TEM images, however, we got one single image showing thread-like fibres of ~ 2.5 nm diameter among typical fibrils (see ESI† S5). The fibres are probably elementary strands of which the ribbons are made. Isolation of the elementary strands would be promising, because it can simplify the construction of a molecular packing model of J-aggregates, which is hopelessly complicated at present. Unfortunately, a controlled decomposition of ribbons has not been possible so far. In this context it must be mentioned, however, that even the molecular packing structure of the cylindrical J-aggregates of the homologue PIC-Cl,[43] is still a topic of discussions despite numerous experimental and theoretical studies over seven decades of research.

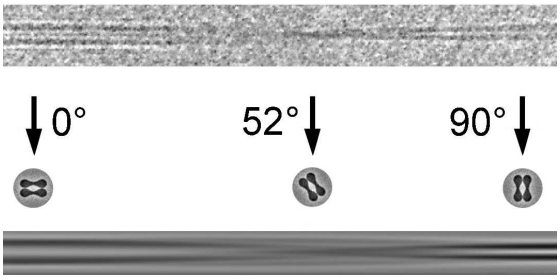

Fig. 11 Cryo-TEM image of a segment (0° − 90°) of a twisted fibrillar J-aggregate (above) and simulated projection image (below). For the simulation a fibril cross-sectional structure was assumed according to Fig. 10d, which consists of a stacked pair of ribbons with dumbbell-shaped density profile that are twisted around the fibril axis (middle). Assuming two-fold rotational symmetry, superposition of the individual cross-sections yields the projection image as shown below.

The aging of dye solutions for several months is accompanied by notable morphological changes. Tubular H-aggregates and fibrillar J-aggregates can no longer be detected and are replaced by broad tape-like aggregates. A representative cryo-TEM micrograph of a two months old sample is shown in Fig. 12 (for an additional example see ESI† S6). The typical width of the tapes ranges between 100 and 200 nm (panel a). A line-scan across the tape in edge-on orientation yields a thickness of 9.0 ± 1.0 nm and a density profile (Fig. 12c) that is nearly identical with that of a single fibril in the 0° orientation (i.e. parallel to the stacking direction; Fig. 10b). Horizontally embedded tapes often show a pattern of striations oriented parallel to the long axis of the tapes. The Fourier transform yields a

value of ~ 2.7 nm (Fig. 12b) for the line spacing, which agrees well with the stacking distance of the dumbbell-shaped ribbons in the fibrils (Figs. 10c,d). The excellent consistence of the respective density profiles (Figs. 10b and 12c) as well as the agreement of the ribbon's stacking distance and the line spacing of tapes suggest that the tapes have been formed by the lateral stacking of individual fibrils as sketched Fig. 12d. While the lateral growth of ribbons accompanied by the stacking into multilayers is often observed in self-aggregating dye systems,[30] the hierarchical organization of PCYN-Cl tapes is different. Here a solely lateral two-dimensional face-to-face assembly process is found.

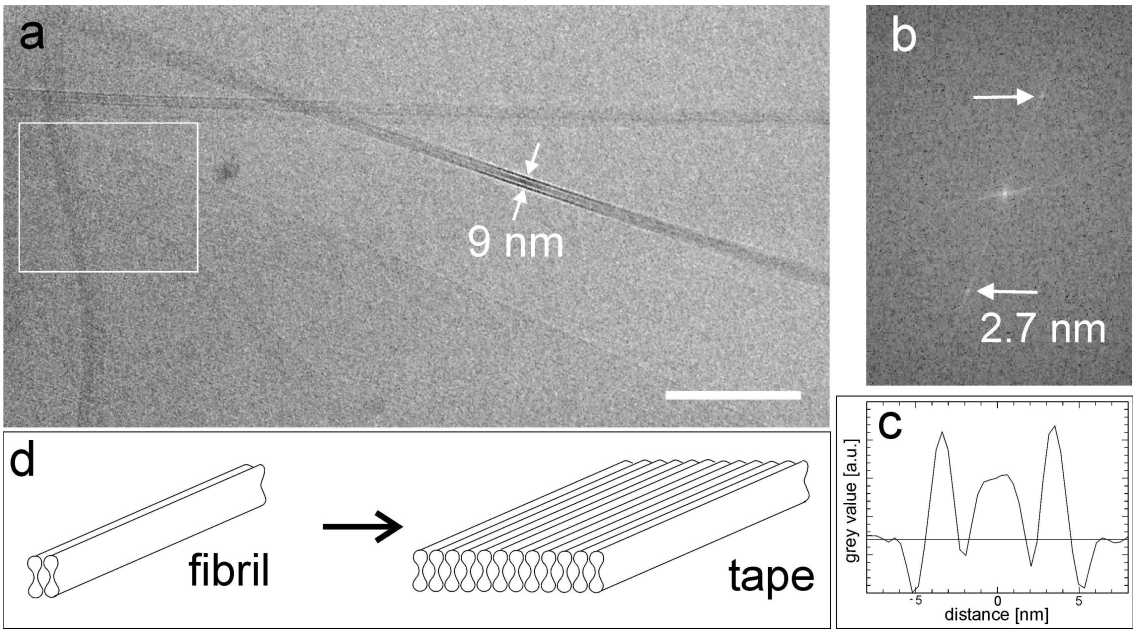

Fig. 12 Cryo-TEM micrograph (a) of an aged solution taken at 0.6 µm defocus. Broad tape-like J-aggregates can be seen. In edge-on orientation the thickness of tapes can directly be estimated. A pattern of fine lines becomes visible in horizontal orientation. The Fourier transform (panel b) taken of the boxed region in panel (a) yields for the spacing of lines a value of ~ 2.7 nm. (c) Grey value profile of a tape in edge-on orientation. (d) Schematic illustrating the structural transformation of fibrils into tapes. Sample: 1.0 mM PCYN-Cl solution stored in the dark for two months. Bar = 100 nm.

4. Conclusions

Detailed spectroscopic and morphological investigations have been performed to characterize the process of aggregation of PCYN-Cl in aqueous solutions in a concentration range from 50 µM up to 1 mM. H-type dimers and oligomers probably exist at a concentration of ~ 0.35 mM, but they were expectedly too small to be visualized by cryo-TEM. Above 0.7 mM, however, several hundreds of nanometre long tubular H-aggregates became visible.

Spectroscopically they are characterized by a broad and nearly symmetric absorption band centred at around ~ 511 nm. These findings confirm a recent SAXS study of pinacyanol acetate liquid crystalline phases, which inferred tubular aggregates at much high concentration as well. Linear dichroism spectra suggest, however, that the monomers forming the single layered wall of PCYN-Cl nanotubes are oriented mainly parallel to the tube axis, precluding the proposed hollow brickwork chimney structure as molecular packing model.

The detected tubular H-aggregates proved to be unstable. When the dye concentration exceeds 0.7 mM they transform into J-aggregates. Though precipitation was observed at around 10 mM solid crystals have not been identified and the precipitated material presumably consists of agglomerated aggregates. J-aggregation shows a pronounced long-time kinetics and a dependency on the route of sample preparation. In particular, the application of shear can markedly accelerate the transformation and proved to be the simplest way to produce J-aggregates. The J-aggregates possess a split absorption spectrum composed of two longitudinally polarized J-bands and one H-band that is polarized perpendicular to the aggregate axis. The J-aggregates become visible in the optical microscope as thread-like, flexible, and many tens of micrometers long fibres. Cryo-TEM reveals their highly complex ultrastructure. In freshly prepared solutions the J-aggregates consist mainly of ~ 9 nm wide fibrils, which are composed of a pair of ribbons with dumbbell-shaped density cross-sections that are stacked face-to-face and twisted around the fibril axis. Upon aging they unilaterally stack face-to-face to form tens of nanometres wide and ~ 9 nm thick tape-like aggregates.

The detection of H- and J-aggregates of mesoscopic size was not expected for PCYN-Cl. This finding makes the dye appear more comparable to the shorter homologue PIC-Cl, which in aqueous solution forms micrometer long thread-like J-aggregates. Compared to these the J-aggregates of PCYN-Cl possess a much more complex morphology making them interesting for further investigations in order to study the relation between optical properties and supramolecular architecture.

References

(1) F. Würthner, T. E. Kaiser and C. R. Saha-Möller, *Angew. Chem. Int. Ed.*, 2011, **50**, 3376.

(2) M. Kasha, H. R. Rawls and M. Ashraf El-Bayoumi, *Pure Appl. Chem*., 1965, **11**, 371.

(3) V. Czikkely, H. D. Försterling and H. Kuhn, *Chem. Phys. Lett*., 1970, **6**, 11.

(4) V. Czikkely, H. D. Försterling and H. Kuhn, *Chem. Phys. Lett*., 1970, **6**, 207.

(5) E. E. Jelly, *Nature*, 1936, **138**, 1009.

(6) G. Scheibe, *Angew. Chem*., 1937, **50**, 51.

(7) T. Tani, *Photographic Sensitivity; Theory and Mechanisms*, Oxford University Press, New York, 1995.

(8) T. Kobayashi, *J-Aggregates*, World Scientific, Singapore, 1996.

(9) K. D. Volkova, V. B. Kovalska, A. O. Balanda, R. J. Vermeij, V. Subramaniam, Yu. L. Slominskii and S. M. Yarmoluk, *J. Biochem. Biophys. Methods*, 2007, **70**, 727.

(10) Z. Zhang, J. Fan, P. P. Cheney, M. Y. Berezin, W. B. Edwards, W. J. Akers, D. Shen, K. Liang, J. P. Culver and S. Achilefu, *Molec. Pharmac*., 2009, **6**, 416.

(11) M. H. Robbins and R. S. Drago, *J. Catal*., 1997, **170**, 295.

(12) S. Barazzouk, H. Lee, S. Hotchandani and P. V. Kamat, *J. Phys. Chem. B*, 2000, **104**, 3616.

(13) W. A. Adeagbo, V. Buss and P. Entel, *J. Incl. Phenom. Macrocycl. Chem*., 2002, **44**, 203.

(14) A. K. Panda and A. K. Chakraborty, *J. Photochem. Photobiol. A*, 1997, **111**, 157.

(15) S. J. Khouri and V. Buss, *J. Biophys. Chem*., 2011, **2**, 380.

(16) S. J. Khouri, D. Richter and V. Buss, *J. Incl. Phenom. Macrocycl. Chem*., 2009, **65**, 287.

(17) R. Sabaté, M. Gallardo and J. Estelrich, *J. Colloid Interf. Sci*., 2001, **233**, 205.

(18) S. J. Khouri and V. Buss, *Open J. Phys. Chem*., 2012, **2**, 34.

(19) K. Kostarelos, P. F. Luckham and T. F. Tadros, *J. Colloid Interf. Sci*., 1997, **191**, 341.

(20) R. Sabaté and J. Estelrich, *Biopolymers* , 2003, **72**, 455.

(21) R. C. Merrill and R. W. Spencer, *J. Am. Chem. Soc*., 1950, **72**, 2894.

(22) E. K. Batchelor, S. Gadde and A. E. Kaifer, *Supramol. Chem*., 2010, **22**, 40.

(23) W. West and S. Pearce, *J. Phys. Chem*., 1965, **69**, 1894.

(24) H. Min, J. Park, J. Yu and D. Kim, *Bull. Korean Chem. Soc*., 1998, **19**, 650.

(25) S. J. Khouri and V. Buss, *J. Solution Chem*., 2010, **39**, 121.

(26) A. Nemeth, V. Lukeš, J. Sperling, F. Milota, H. F. Kauffmann and T. Mančal, *Phys. Chem. Chem. Phys.*, 2009, **11,** 5986.

(27) N. Christensson, F. Milota, J. Hauer, J. Sperling, O. Bixner, A. Nemeth and H. F. Kauffmann, *J. Phys. Chem. B*, 2011, **115**, 5383.

(28) C. Rodríguez-Abreu, C. A. Torres and G. J. T. Tiddy, *Langmuir*, 2011, **27**, 3067.

(29) C. Böttcher, in *Analytical Methods in Supramolecular Chemistry*, ed. C. A. Schalley, Wiley-VCH, Weinheim, 2nd edn., 2012, vol. 2, ch. 14, pp. 629-709.

(30) H. v. Berlepsch and C. Böttcher, in *J-Aggregates*, ed. T. Kobayashi, World Scientific, Singapore, 1st edn., 2012, vol. 2, ch. 4, pp. 119-153.

(31**)** R. Marrington, T. R. Dafforn, D. J. Halsall, J. I. MacDonald, M. Hicks and A. Rodger, *Analyst*, 2005, **130**, 1608.

(32) H. Mustroph, K. Reiner, J. Mistol, S. Ernst, D. Keil and L. Hennig, *ChemPhysChem*, 2009, **10**, 835.

(33) A. Aggeli, I. A. Nyrkova, M. Bell, R. Harding, L. Carrick, T. C. B. McLeish, A. N. Semonov and N. Boden, *Proc. Natl. Acad. Sci. USA*, 2001, **98**, 11857.

(34) H. von Berlepsch, S. Kirstein, R. Hania, A. Pugžlys and C. Böttcher, *J. Phys. Chem. B*, 2007, **111**, 1701.

(35) S. Ogi, K. Sugiyasu, S. Manna, S. Samitsu and M. Takeuchi, *Nature Chemistry*, 2014, **6**, 188.

(36) G. Garab and H. van Amerongen, *Photosynth. Res*., 2009, **101**, 135.

(37) C. F. Schmid and D. J. Klingenberg, *Phys. Rev. Lett*., 2000, **84**, 290.

(38) A. Onuki, *J. Phys. Condens. Matter*, 1997, **9**, 6119.

(39) H. v. Berlepsch and C. Böttcher, *Langmuir*, 2013, **29**, 4948.

(40) Y. Talmon, *Ber. Bunsenges. Phys. Chem*., 1996, **100**, 364.

(41) G. J. T. Tiddy, D. L. Mateer, A. P. Ormerod, W. J. Harrison and D. J. Edwards, *Langmuir*, 1995, **11**, 390.

(42) H. v. Berlepsch, M. Regenbrecht, S. Dähne, S. Kirstein and C. Böttcher, *Langmuir*, 2002, **18**, 2901.

(43) H. v. Berlepsch, C. Böttcher and L. Dähne, *J. Phys. Chem. B*, 2000, **104**, 8792.